PCCP

Accepted Manuscript

ROYAL SOCIETY OF CHEMISTRY

www.rsc.org/pccp

PCCP

ARTICLE

Aggregation of α-crystallins in kynurenic acid-sensitized UVA photolysis under anaerobic conditions

Received 00th January 20xx,
Accepted 00th January 20xx

DOI: 10.1039/x0xx00000x

www.rsc.org/

P. S. Sherin,[a,b,†] E. A. Zelentsova,[a,b] E. D. Sormacheva,[a,b] V. V. Yanshole,[a,b] T. G. Duzhak,[a,b] and Yu. P. Tsentalovich[a,b]

The reactions of photoexcited kynurenic acid (KNA) with bovine α-crystallins under anaerobic conditions proceed via the electron transfer from tryptophan (Trp) and tyrosine (Tyr) residues to the triplet KNA molecules. The subsequent radical reactions lead to the protein aggregation and insolubilization. The absorption of the photolyzed proteins at 335 nm as well as their total fluorescence significantly increases, while the tryptophan-related fluorescence decreases. It has been established that the alterations of the protein optical properties are related to the modifications of Trp residues. Intrinsic lens antioxidants ascorbate (Asc) and glutathione (GSH) that are present in the human lens at millimolar level effectively block the formation of the observed light-induced protein modifications. The protective effect of Asc was attributed to its ability to quench highly reactive triplet states, while the role of GSH, most likely, corresponds to the reduction of photochemically formed radicals into a diamagnetic state. The results obtained disclose the possible mechanism of UVA-induced modifications of the lens crystallins, leading to the formation of cataract, and the role of major lens antioxidants Asc and GSH in the protection of the lens proteins.

1 Introduction

The main functions of the eye lens are the transmitting and focusing of the incident light onto retina. The dense packing of lens fiber cells and homogeneous distribution of the major lens proteins, crystallins, inside cells provide the transparency of the lens in the visible region and the high refractive index. Crystallins have negligible turnover during the lifespan of an individual; they gradually accumulate numerous post-translational modifications (PTMs), including oxidation, deamination, racemization, truncation, etc.[1-5] These PTMs eventually lead to the formation of large water-insoluble protein aggregates able to scatter the incident light, and thereby to the development of age-related cataract. UV light is often considered as one of the sources of age-related PTMs able to give a substantial contribution to the cataract development.[6-8]

Solar UV radiation reaching the surface of our planet consists of more than 95% of UVA light (320-400 nm) and less than 5% of UVB (280-320 nm) and shorter wavelength radiation. Though UVB light has deleterious effect on the protein structure and functionality, its major part is absorbed in the cornea,[9] while UVA radiation is able to penetrate deep into the human lens.[7,10] Long-term exposure of animal models to UVA radiation results in the crystallin aggregation in the lens nucleus and the augmentation of the light scattering.[11-14] A significant role of UVA radiation in the skin photoaging and carcinogenesis has also been reported.[15,16] These observations indicate the importance of UVA radiation in the development of the eye and skin diseases.

Normally proteins do not absorb UVA radiation, but this radiation can be absorbed by endogenous chromophores of a tissue. Photoexcited chromophores (mainly in the triplet state) can either react with proteins directly (Type I of photosensitized oxidation) or modify them via the generation of reactive oxygen species, ROS (Type II).[16,17] The majority of previous works concerned with the protein photooxidation in the presence of chromophores were performed under aerobic conditions[18-25], with few exceptions.[26-28] Taking into account that the concentration of molecular oxygen in the human lens is extremely low (< 2 μM)[29], aerobic conditions seem to be far from the physiological ones. Photochemical damages of the lens proteins under anaerobic conditions are more relevant to the processes taking place in the real lens tissue.

The main chromophores of the human lens in UVA region are kynurenine (KN, Chart 1) and its derivatives.[30-34] These natural metabolites of amino acid tryptophan are believed to act as molecular UV filters because of the low yields of reactive triplets (below 1%)[34-36] and high photochemical stability.[34,36] However, in our previous works it has been shown that the triplet KN can be quenched by amino acids tryptophan and tyrosine and antioxidant ascorbate (Asc) via the electron transfer to KN.[37] Thus, in the lens the photoexcited KNs can initiate the photooxidation of crystallins, and the intrinsic antioxidant Asc can prevent these undesirable reactions.

Under physiological conditions, the natural UV filters undergo the reactions of thermal or photochemical degradation.[38,39] The resulting products include the covalent binding of KNs to

[a] International Tomography Center of Siberian Branch of Russian Academy of Science, Intitutskaya str. 3A, 630090, Novosibirsk, Russia.
[b] Novosibirsk State University, Pirogova str. 2a, 630090, Novosibirsk, Russia.
† Corresponding author: Tel. +7-383-330-54-29, e-mail: sherin@tomo.nsc.ru.
Electronic Supplementary Information (ESI) available: [details of any supplementary information available should be included here]. See DOI: 10.1039/x0xx00000x

lens proteins,[40,41] the formation of "secondary UV filters"[34,36,38,40] and the generation of cyclized products such as KN yellow,[38] 4-hydroxyquinoline (4HQN)[39] and kynurenic acid (KNA, Chart 1).[42-44] KNs covalently bound to proteins and the cyclized products exhibit higher triplet yields and lower photochemical stability as compared to the parent UV filters.[34,45-47] In particular, 4HQN and KNA demonstrate high photosensitizing abilities: the yields of reactive triplet states are 35% for 4HQN[45] and 80% for KNA[47]. To the best of our knowledge, there are no reports on the 4HQN content in the human lens. KNA was found in the normal human lens at the levels of 1-2 μM/mg,[44] which is two orders of magnitude lower than the total concentration of UV filters, ≈ 400-600 μM/mg.[31,32,48] Taking into account that the triplet quantum yield for KNA is two orders of magnitude higher than for KNs, one can presume that UVA irradiation of a lens would result in the generation of similar quantities of KNA-derived and UV filter-derived reactive triplet species. Therefore, the photochemical reactions of KNA and KNs with the lens proteins might give comparable contributions to the total photoinduced modifications of crystallins. In cataractous lenses, the levels of intrinsic UV filters decrease,[32,48-50] while the level of KNA significantly increases,[44] which should elevate the contribution of KNA in photoinduced modifications of crystallins.

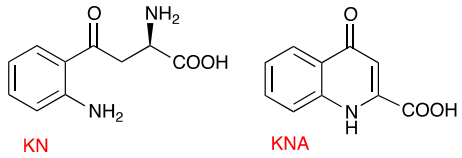

Chart 1. Chemical structures of KN and KNA.

The main purpose of the present work is to shed light on the mechanisms of UVA induced modifications of the lens crystallins caused by photoexcited chromophores under anaerobic conditions. For this purpose we used KNA, which has much higher triplet quantum yield than KNs. This gives the opportunity to significantly reduce the irradiation dose and, therefore, to minimize the contribution from secondary photochemistry of photolytic products. The goals of the work are: (i) to study the mechanisms of modifications of the major lens protein, α-crystallin, induced by photoexcited triplet KNA and (ii) to investigate the role of the lens intrinsic antioxidants, Asc and glutathione (GSH), in the prevention of protein photodamage. Both Asc and GSH are the most abundant lens antioxidants; in the human lens, their concentrations are in the range of 1-10 mM.[31,51] GSH does not directly react with KN triplets,[37] but it is a well-known radical scavenger,[52,53] which can deactivate the radicals formed in photoinduced reactions. Therefore, GSH can also play an important role in the prevention of protein modifications.

2 Results

2.1. Flash-photolysis study of ^{T}KNA reactions

2.1.1. Reactions of ^{T}KNA with amino acids

The optical excitation of KNA in neutral aqueous solution results in the formation of ^{T}KNA triplet state with the absorption maximum at 600 nm.[47,54] In the absence of quenchers, the major channel of the triplet state decay is the triplet-triplet annihilation proceeding with $k_{T\text{-}T}/\varepsilon_{600} = 4.6\times10^{5}$ cm s^{-1}.[47] In the presence of triplet quenchers, the triplet state decay monitored at 600 nm becomes exponential, the observed pseudo-first order rate constant k_{obs} being proportional to the quencher concentration:

$$k_{obs} = k_0 + k_q \times C_q \quad (1)$$

where k_q is the quenching rate constant, and C_q is the quencher concentration. The rate constants of the triplet KNA quenching by amino acids tryptophan (Trp), tyrosine (Tyr) and cysteine (Cys), by oxygen and by antioxidants Asc and GSH were measured for two types of solvents: PBS and PBS containing 6 M urea. The k_q values were determined from the linear approximation of the $k_{obs}(C_q)$ dependences (see Figure S1 of Supporting Information, SI) according to the equation (1); the obtained values are listed in Table 1. The measurements performed in the presence of other amino acids (histidine, phenylalanine, methionine) did not reveal any acceleration of the ^{T}KNA decay. The rate constants of the ^{T}KNA quenching in the presence of 6 M urea are approximately 1.5-2 fold lower than that in PBS solution. This effect should be attributed to the viscosity augmentation by a factor of 1.5 for 6 M urea aqueous solution.[55]

Transient absorption spectra recorded in the photolysis of 3.3×10^{-4} M KNA with 1.0×10^{-3} M Trp (circles) and 1.0×10^{-3} M Tyr (squares) in PBS / 6 M urea solution are shown in Figure 1. The spectra were obtained after the completion of the triplet KNA decay (37 μs after the laser flash), so they correspond to the radicals formed in the quenching reaction: $Trp^{\bullet}$ (absorption maximum at 510 nm)[56-58], $Tyr^{\bullet}$ (maximum at 410 nm)[57] and $KNA^{\bullet}$. The most probable mechanism of the reaction of ^{T}KNA quenching by aromatic amino acids is the electron transfer followed by the deprotonation of $Trp^{\bullet+}$ and $Tyr^{\bullet+}$ cation radicals. However, the possibility of the hydrogen atom transfer also cannot be ruled out.

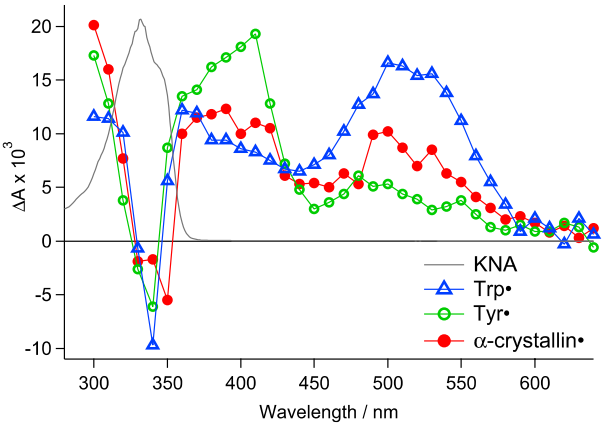

Figure 1. Transient absorption spectra obtained in 355 nm photolysis of 3.3×10^{-4} M KNA in argon-saturated PBS / 6 M urea solution 37 μs after the laser flash: blue triangles – in the presence of 1.0×10^{-3} M Trp; green circles – in the presence of 1.0×10^{-3} M Tyr; red circles – in the presence of 2.8 mg ml^{-1} α-crystallin. Grey line: steady state absorption spectrum of KNA in PBS / 6 M urea solution.

2.1.2. Reactions of ^{T}KNA with α-crystallin

The preliminary experiments on the KNA photolysis in the presence of α-crystallin were performed in PBS; however, no ^{T}KNA quenching by α-crystallin has been observed with the protein concentration up to 12 mg ml^{-1}. In aqueous solution, α-crystallin monomers form large multimers with the molecular masses of 800-1200 kDa. Each such multimer contains approximately fifty α-crystallin monomers, so the molar concentration of multimers is fifty times lower than that of α-crystallin monomers. Under such conditions, the triplet-triplet annihilation becomes the major channel of the triplet decay, and the observation of ^{T}KNA quenching by α-crystallin in its native state might be possible only at a very high protein concentration, which is technically difficult to obtain. For this reason, the measurements were performed in the presence of a denaturing agent (6 M urea), which inhibits the protein multimer formation. The denatured α-crystallin quenches ^{T}KNA with the rate constant of (9.4±0.9)×10^{8} M^{-1}s^{-1}. The $k_{obs}(C_q)$ dependence on the protein concentration is shown in Figure S1, SI. The transient absorption spectrum obtained after the completion of the triplet KNA decay (37 μs after the laser flash) is shown in Figure 1. This spectrum demonstrates the presence of both Trp$^{\bullet}$ and Tyr$^{\bullet}$ oxidized residues in the protein.

It is important to notice that the subsequent decay of radicals observed in the photolysis of KNA with Trp, Tyr and α-crystallin does not result in the formation of new absorption bands. This testifies that the major pathway of the radical decay is the back electron transfer, leading to the restoration of the initial compounds.

2.2. Photoinduced modifications of α-crystallin

2.2.1. Steady-state absorption and fluorescence spectra

The samples containing 6.0 mg ml^{-1} α-crystallin and 3.0×10^{-4} M KNA in PBS solution were photolyzed with the mercury lamp for 20 minutes. The aliquots of photolyzed samples were purified from low-molecular-mass compounds, and the UV-Vis absorption spectra were recorded for purified proteins in PBS solutions. Figure 2A shows the normalized absorption spectra of α-crystallin photolyzed in the absence of antioxidants. The appearance of a band at ca. 335 nm indicates the formation of UVA-absorbing modifications. The presence of 2mM Asc or 2 mM GSH during the UVA photolysis significantly reduces the intensity of this band in the absorption spectrum (Figure 2B, green and blue lines).

The UVA photolysis was also carried out in the presence of 6 M urea in order to compare the character of modifications induced by the reactions of ^{T}KNA with α-crystallin in multimeric and monomeric forms. The absorption spectrum of purified α-crystallin photolyzed under urea-denaturing conditions shows the formation of a similar absorption band in UVA region (Figure 2B, violet line), though the shape of this

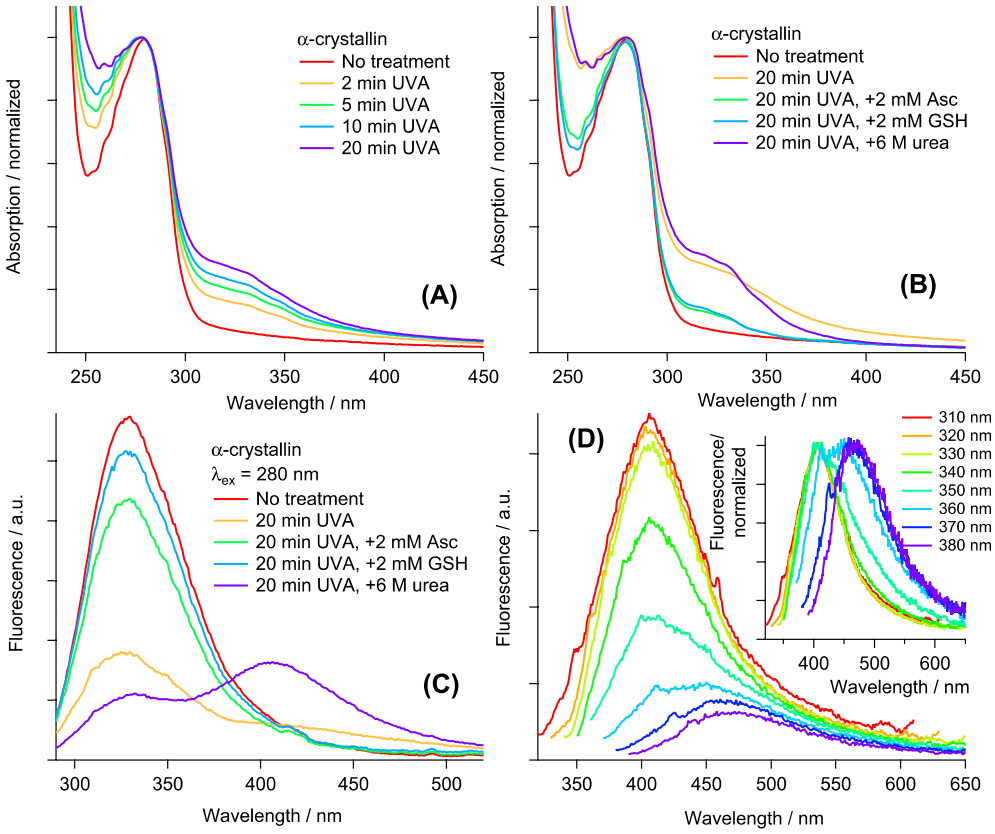

Figure 2. (A-B): Normalized absorption spectra of purified α-crystallin in PBS solution (A) after different time intervals of KNA-sensitized UVA photolysis and (B) after 20 min of KNA-sensitized UVA photolysis in the absence and presence of antioxidants or 6 M urea. (C-D): Fluorescence emission spectra of purified α-crystallin (C) after 20 min of KNA-sensitized UVA photolysis in the absence and presence of antioxidants or 6 M urea recorded with the excitation at 280 nm and (D) after 20 min of KNA-sensitized UVA photolysis recorded with various excitation wavelengths. Inset in (D): the same data after normalization.

band slightly differs from the spectrum of α-crystallin photolyzed under native conditions (Figure 2B, orange line).

The purified proteins were also subjected to fluorescence measurements. The fluorescence emission spectra of α-crystallin before and after 20 min of UVA photolysis under native and urea-denaturing conditions as well as in the absence and presence of antioxidants were recorded with the excitation at 280 nm (Figure 2C). A significant decrease of the Trp-related emission band with the maximum at 330 nm and the formation of a new emission band at ca. 405 nm are the main changes in the fluorescence properties of proteins. These changes are much smaller in the presence of antioxidants, but they become more pronounced in the presence of 6 M urea (Figure 2C and Figure S2 of SI).

The fluorescence emission spectra recorded with the excitation across the new band at ca. 335 nm are presented in Figure 2D. The emission spectra after normalization (inset in Figure 2D) clearly show the presence of two emission bands with the maxima at ca. 405 and 470 nm, which should be attributed to at least two types of modifications with the different fluorescence properties. Thus, both absorption and fluorescence data demonstrate the formation of fluorescent modifications whose spectral properties markedly differ from that of Trp and Tyr residues.

2.2.2. SDS-PAGE analysis

Figure 3A shows sodium dodecyl sulfate polyacrylamide gel electrophoresis (SDS-PAGE) of α-crystallin after KNA-sensitized UVA photolysis. Lanes 2-6 correspond to PBS solutions and lane 7 – to PBS / 6 M urea solution. Lane 2 represents the untreated sample, lane 3 – the sample bubbled with argon for 20 minutes, and lanes 4-6 – the samples subjected to UVA photolysis under argon bubbling for 20 minutes. The irradiation of the sample in lane 5 was performed in the presence of 2 mM Asc, and of the sample in lane 6 – in the presence of 2 mM GSH. The difference between the samples in the lanes 2 and 3 is negligible which indicates a minor impact of argon bubbling on the integrity of protein. The control measurements performed with the UVA photolysis of α-crystallin in PBS in the absence of KNA also did not reveal any changes in the protein structure (Figure S3 of SI).

The formation of covalently bound aggregates with high molecular masses (> 40 kDa) is the major change in the protein structure after 20 minutes of UVA photolysis (lane 4, Figure 3A). The photolysis in the presence of 6 M urea results in the extensive aggregate formation and almost complete vanishing of α-crystallin monomers (lane 7, Figure 3A). The aggregate formation is completely inhibited by the presence of Asc or GSH (lanes 5 and 6, Figure 3A). The aggregates so formed are resistant to β-mercaptoethanol treatment indicating that the bonds between the monomers are not the disulfide bridges. The proteins from α-crystallin family contain only one cysteine residue (Cys131 of αA-crystallin), so the extensive aggregation via the disulfide bridges is not expected. The α-crystallin dimers linked by disulfide bridges do exist in the starting material, but their abundance does not increase with irradiation (Figure S4 of SI).

Figures 3B and 3C demonstrate the kinetics of α-crystallin photolysis in the presence of KNA under argon bubbling in PBS and PBS / 6 M urea solutions, respectively. A consecutive formation of dimers and higher oligomers can be clearly seen. This testifies that the aggregation does not lead to an immediate loss of solubility of the forming oligomers, which continue to grow in size with the dose of UVA radiation. A significant acceleration of the α-crystallin aggregation under urea-denaturing conditions should be attributed to the loss of the protein spatial self-organization and, correspondingly, to the better accessibility of Trp- and Tyr-residues for the reactions with ^{T}KNA, and of modified residues for cross-linking.

The protein-containing bands were excised from gels and subjected to the in-gel tryptic digestion followed by matrix assisted laser desorption/ionization time-of-flight (MALDI-TOF) and high performance liquid chromatography electrospray ionization (HPLC-ESI) mass spectrometry (MS) analyses of the obtained peptides. It was found that all bands contain the mixtures of αA- and αB-crystallins or their fragments with a minor inclusion of β-crystallins.

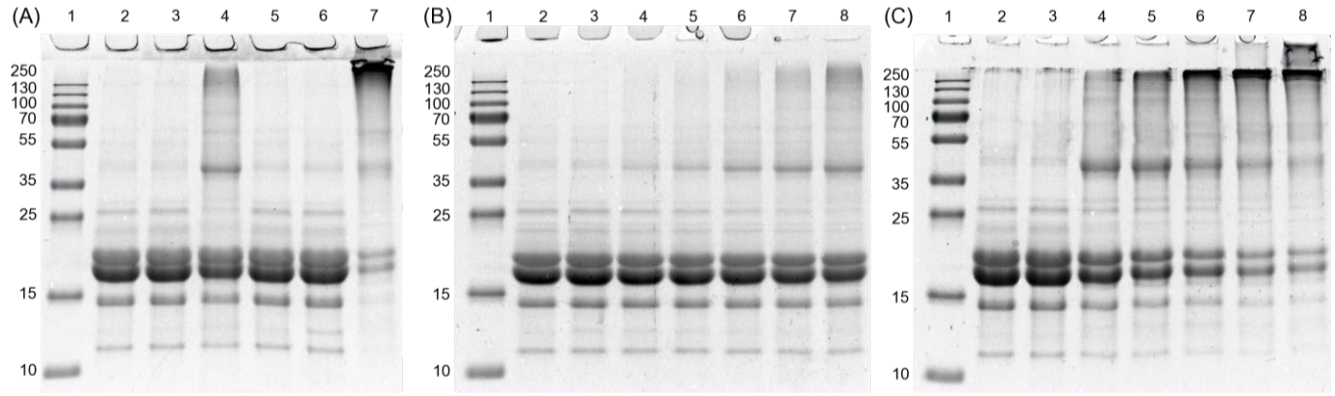

Figure 3. 15% SDS-PAGE of α-crystallin after KNA-sensitized UVA photolysis. (A-C): Lane 1 – molecular mass standards (kDa); lane 2 – α-crystallin without any treatment; lane 3 – after 20 min of argon bubbling. (A): PBS, lane 4 – 20 min of photolysis without antioxidants; lane 5 – 20 min of photolysis in the presence of 2 mM Asc; lane 6 – 20 min of photolysis in the presence of 2 mM GSH; lane 7 – 20 min of photolysis in the presence of 6 M urea. (B): PBS, lanes 4-8: 1, 2, 5, 10, and 20 min of photolysis.
(C) PBS, 6 M urea, lanes 4-8: 1, 2, 5, 10, and 20 min of photolysis.

2.2.3. HPLC-ESI-MS analysis of tryptic peptides from photolyzed α-crystallins

2.2.3.1 Degradation of starting material

The purified aliquots of α-crystallins were subjected to the in-solution tryptic digestion and analyzed by HPLC-ESI-MS. The absorption of peptides obtained from irradiated and non-irradiated samples at 220 nm as well as the intensities of MS signals were similar. This indicates the successful enzymatic hydrolysis of large α-crystallin aggregates formed under UVA radiation.

The quantitative analysis was performed for 18 peptides corresponding to αA-crystallin and 18 peptides corresponding to αB-crystallin (two of them were common, so the total number of the analyzed peptides was 34). The abundance of each peptide in the samples was determined by the integration of peak areas in the Extracted Ion Chromatogram (extraction window ±0.01 Da) obtained for this peptide. It was assumed that the initial peptide molar concentrations (before irradiation) are equal to the initial molar concentrations of αA- or αB-crystallins present in the solution at 3:1 ratio obtained from the HPLC-ESI-MS analysis of the intact α-crystallin mixture extracted from the bovine lens. It was found that the abundances of 18 peptides (8 peptides of αA-crystallin and 10 peptides of αB-crystallin) do not change under UVA radiation; at the same time, the abundance of all Trp- and Tyr-containing peptides decreases with the irradiation dose. Figure 4A and 4B shows the decay of αA-crystallin peptides, residues 1-11 (Trp9) and 104-112 (Tyr110); the presented data are the mean values for three independent experiments on the KNA-sensitized UVA photolysis of α-crystallin.

The dynamics of other Trp- and Tyr-containing peptides can be found in SI (Figure S5). The presence of antioxidants prevents the peptide degradation (data for GSH are not shown). These results are in a good agreement with the optical data (Figure 2) and SDS-PAGE data (Figure 3).

2.2.3.2 Formation of photoinduced products

The major modifications revealed by MS and MS/MS analysis of tryptic digests of the photolyzed α-crystallin are: (i) +15.995 Da at Met1 of αA- and αB-crystallin and at Met68 of αB-crystallin; (ii) −2.017 Da at Trp9 of αA- and αB-crystallin and at Trp60 of αB-crystallin; (iii) +15.995 Da at Trp9 of αA- and αB-crystallin and at Trp60 of αB-crystallin; (iv) +31.988 Da at Trp9 of αA-crystallin. The abundances of peptides containing these modified residues increase with UVA radiation dose as illustrated in Figures 4(C-E) and S7 of SI. MS/MS spectra of the 1-11 peptide of αA-crystallin (N-term acetylated) with oxidized Met1 (+15.995 Da) and modified Trp9 (−2.017 Da) are shown in Figure 5; MS/MS data for other peptides can be found in SI.

Methionine oxidation is one of the most common PTMs accumulated in the lens crystallins.[59] Besides, the methionine residues might be oxidized during the sample preparation.

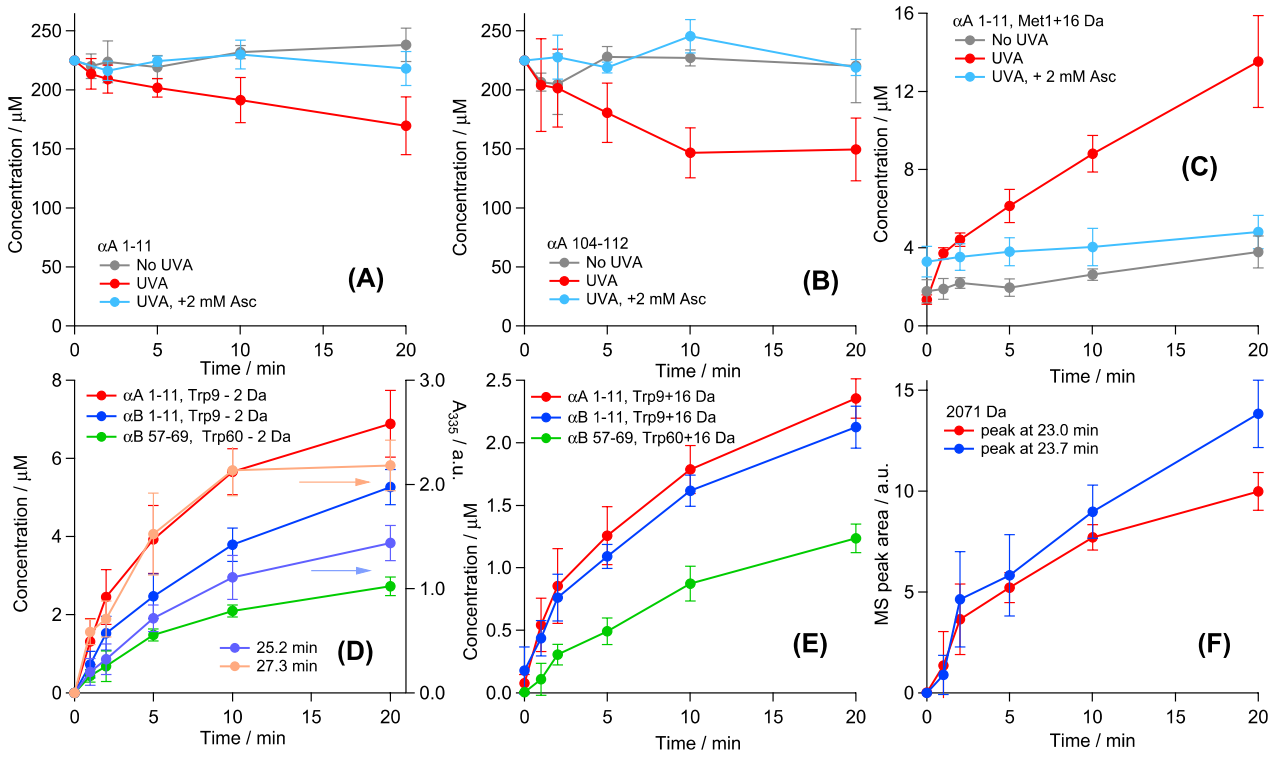

Figure 4. (A-C): Time dependences of concentrations of αA-crystallin peptides: (A) residues 1-11 (Trp9); (B) residues 104-112 (Tyr110); (C) residues 1-11 with oxidized Met1. Grey circles – control non-irradiated sample; red circles – KNA-sensitized UVA photolysis; blue circles – the same photolysis in the presence of 2 mM Asc. (D, E): Time dependences of concentrations of 1-11 residues of αA-crystallin peptide (red circles), residues 1-11 (blue circles) and 57-69 (green circles) of αB-crystallin peptides with modified Trp residues: (D) −2.017 Da and (E) +15.995 Da. Light blue and pink lines in (D) are the time dependences of absorption at 335 nm corresponding to peaks eluted at 25.2 and 27.3 min, respectively. (F): Time dependences of MS peak area corresponding to a peptide with mass of 2071.046 Da eluted as two peaks at 23.0 and 23.7 min. Each point is the average value ± standard deviation of three independent experiments.

Indeed, all starting samples contain some amounts of these peptides (Figure 4C and S6A, S6B of SI). However, the abundances of these peptides monotonically increase with UVA radiation dose, while in the absence of UVA light their concentrations almost do not change (Figure 4C and S6A, S6B of SI). This clearly demonstrates the photosensitized origin of this modification.

α-Crystallin contains three Trp residues (Trp9 in αA-crystallin and Trp9, Trp60 in αB-crystallin), and the −2.017 Da modification was found for all three Trp-containing peptides. The retention time of the modified 1-11 peptide of αA-crystallin is 27.3 min; the modified 1-11 and 57-69 peptides of αB-crystallin co-elute at 25.2 min. These three peptides are characterized by absorption spectra with the maxima at 335 nm (Figure 6). The absorption at 335 nm monitored by the HPLC DAD flow cell, increases with the irradiation dose in the same way as the intensities of MS signals from these peptides (Figures 4D). It should be noted that the peaks eluted at 25.2 and 27.3 min also contain 1-11 peptide of αA- and αB-crystallin and 57-69 peptide of αB-crystallin with the modification of +13.979 Da. Abundances of these three peptides also increase with the dose of UVA radiation (Figure S6C of SI). Unfortunately, the intensities of ions corresponding to these peptides were too low to record the MS/MS spectra. Taking into account that the resulting mass difference of +13.979 can be represented as a sum of two modifications +15.996 and -2.017 Da, these peptides could be tentatively attributed to the oxidized peptides (most likely, at the Met position) of αA- and αB-crystallins with −2.017 Da modification at the Trp residue. The accumulation of peptides with both modifications, −2.017 Da and +13.979 Da, slows down under prolonged irradiation. This probably indicates that they are not the final products, and undergo further reactions. Taking into account the absorbance of these peptides in UVA region (Figure 6), one can presume that these peptides undergo the direct photolysis rather than the KNA-sensitized photolysis.

The single oxidation of Trp residues, +15.995 Da, is another common KNA-sensitized modification for all three Trp-containing peptides (see Figure 4E for the accumulation dynamics and Pages 9, 13, 16 of SI for MS/MS data). Each Trp-oxidized peptide elutes as two peaks (data in Figure 6E correspond to the sum of two peak signals) that probably indicates the oxidation of indole ring at different positions. Double oxidation of Trp residue was confidently observed only for Trp9 of αA-crystallin (Figure S6D and Page 10 of SI). Our data also show the formation of two other doubly oxidized 1-11 peptides of αA-crystallin (Figure S6E of SI). However, the structures of these peptides were not determined because of the low MS signal intensities. Perhaps, they could be attributed to the 1-11 peptides of αA-crystallin with the

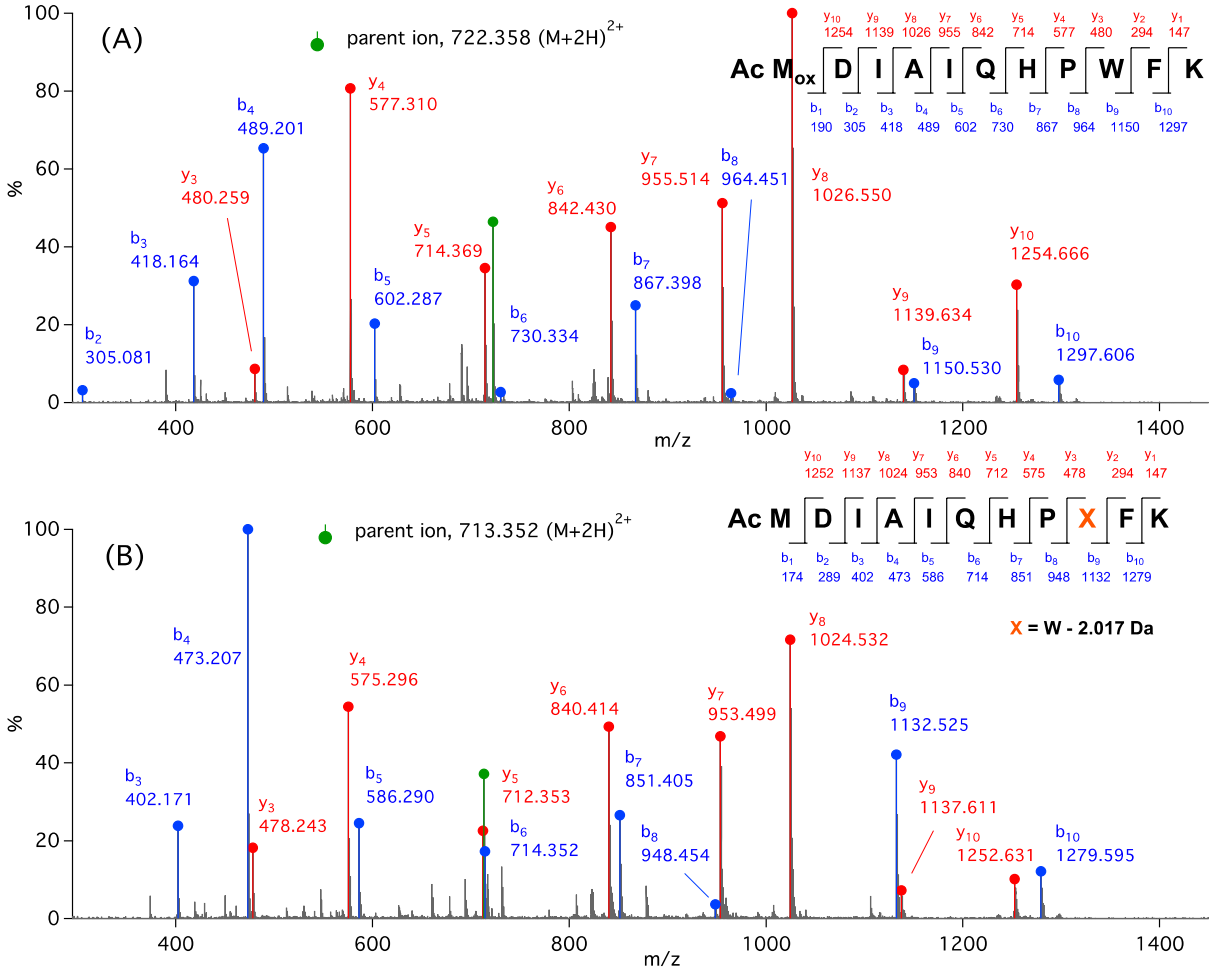

Figure 5. MS/MS spectra of modified peptides of αA-crystallin: (A) residues 1-11 with oxidized Met1; (B) residues 1-11, X denotes modified Trp9 (mass change −2.017 Da).

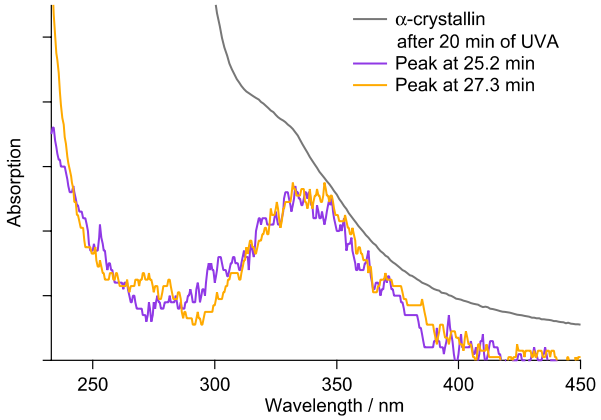

Figure 6. Absorption spectra of peptides eluted at 25.2 min (violet) and 27.3 min (orange) and of the purified α-crystallin (grey) after 20 min of KNA-sensitized UVA photolysis in PBS.

oxidized Met1 and Trp9 residues with different positions of the indole ring oxidation.

The HPLC-ESI-MS data revealed the formation of a peptide with the mass of 2071.046 Da, which matches the mass of a dimer of 13-21 peptide of αA-crystallin (1036.533 Da). This peptide elutes as two peaks of similar intensities; the observed signals monotonically increase during the photolysis (Figure 4F). The photolysis in the presence of 6 M urea yields approximately five-fold higher concentration of this peptide as compared to the irradiation under native conditions. The 13-21 peptide of αA-crystallin contains one Tyr residue (Tyr18); one can presume that the observed peptide is formed via the intermolecular Tyr-Tyr (dityrosine) bonding, which is the well-known intermolecular cross-link of proteins.[17] Unfortunately, low intensity of the MS signal does not allow for the recording of MS/MS spectra to confirm this presumption.

Qualitatively, the photolysis in the presence and absence of urea gives similar results: all modifications found in α-crystallin after the photolysis under native conditions were also observed after the photolysis in the presence of 6 M urea. However, in the presence of urea the abundance of peptides with the −2.017 Da modification at the Trp residues was approximately five times higher, and the abundance of oxidized peptides – approximately 1.5 times higher. Most probably, this difference in the product formation should be attributed to the different availability of amino acid residues for the reactions with ^{T}KNA triplets and KNA$^{\bullet}$ radicals.

The presence of antioxidants during the photolysis prevents the formation of all modifications mentioned above. Thus, both Asc and GSH effectively inhibit the KNA photosensitized modifications of α-crystallins.

It should be noted that the results of MS experiments shown in Figures 4, and S5, S6 of SI should be considered as semi-quantitative ones. The correct quantitative MS measurements require a set of calibration measurements for each compound under study. Due to the absence of standards for peptides of αA- and αB-crystallin, we presumed that the modifications have no influence on the efficiency of the peptide ionization, and both modified and unmodified peptides give MS signals of the same intensity. This presumption is not always true, so the results presented in Figures 4 and S5, S6 of SI demonstrate the qualitative dynamics of the peptide modifications rather than the absolute values of the modified peptide concentrations.

3 Discussion

Harmful influence of UVB irradiation (280-320 nm) on the eye tissues is known for many years. Experiments with the model animals demonstrate that the intense UVB irradiation causes changes in the metabolomic[60,61] and proteomic[19] compositions of the lens and provokes the cataractogenesis.[62,63] Recent investigations have shown that the intense UVA radiation (320-400 nm) also induces oxidation, crosslinking and aggregation of the eye lens proteins.[12-14,21,24-26,64] Varma et al[8] cites rather convincing images of the Earth maps, demonstrating strong correlation between the global level of UV index and the cataract incidence: the excessive solar irradiation in the wavelength region over 300 nm presents a significant risk factor for the cataractogenesis. It should be emphasized that the majority of *in vitro* experiments on the crystallin photolysis were performed under aerobic conditions, i.e. under conditions when the protein modifications occur via the Type II photosensitized mechanism with the formation of ROS.[18-25] The singlet oxygen and oxygen-derived radicals react with the oxidizable amino acid residues (cysteine, histidine, methionine, tryptophan, tyrosine), and the subsequent reactions of the oxidized residues may cause intra- and intermolecular cross-linking.

The idea of the *in vivo* crystallin modifications via the Type II photosensitized mechanism contradicts the report[29] on very low oxygen level in the human lens (< 2 μM). The lifetimes of photoexcited chromophores in the triplet state are limited by the concentration of suitable quenchers present in solution; with the low oxygen level, the direct reactions of photoexcited chromophores with aromatic amino acid residues of crystallins seem to be more plausible. In this work, we present the report on the extensive *in vitro* photoinduced aggregation of α-crystallins under anaerobic conditions without ROS participation (the Type I photosensitized oxidation).

In the human lens, most of UVA light is absorbed by intrinsic UV filters – KN and its derivatives.[30,31] The major decay channel of KN singlet excited state is the internal conversion into the ground state (approximately 99%),[34,65] while the triplet yield is below 1%.[34] In the lens, natural UV filters may be transformed in thermal or photochemical reactions yielding different products,[38,39] including KNA. The latter is characterized by the high yield of triplets[47] and high reactivity toward the aromatic amino acids Trp and Tyr, as shown in ref.[66] and this work. Moreover, the rate constants of the ^{T}KNA quenching by Trp and Tyr are one order of magnitude higher than those for ^{T}KN.[37] Thus, the photochemical reactions of KNA might give a substantial contribution to the photoinduced modifications of the lens crystallins.

In the present work, the study of KNA-sensitized UVA photolysis of α-crystallin under anaerobic conditions was performed by the broad set of methods, including optical spectroscopy, gel-electrophoresis and mass spectrometry. The

obtained results make it possible to propose a general mechanism of α-crystallin modification under anaerobic KNA-sensitized UVA photolysis (see Scheme 1). The photoexcitation of KNA results in the formation of KNA triplet state. Since the rate constants of the ^{T}KNA quenching by Trp and Tyr are much higher than by other amino acids (Table 1), ^{T}KNA reacts with the Trp and Tyr residues of α-crystallin with the formation of Trp$^{\bullet}$ and Tyr$^{\bullet}$ radicals (Figure 1). The unpaired electron may migrate along the polypeptide chain;[67,68] however, in the absence of radical scavengers, the only possible channels of the radical decay are the reactions of recombination or disproportionation with other radicals. Such reactions lead to the protein crosslinking (Figure 3) and to the formation of UVA-absorbing protein modifications (Figures 2 and 6). The reactions leading to the protein crosslinking can be iterated, that results in the formation of covalently linked high molecular mass oligomers (Figures 3B and 3C).

The oxidation of Met and Trp residues under anaerobic photolysis can proceed via two possible mechanisms: (i) the radical reactions between KNA$^{\bullet}$ and amino acid residues resulting in the oxygen transfer from KNA to a residue; or (ii) the photosensitized oxidation via Type II reactions of ^{T}KNA with the residual oxygen present in solution. In the latter case, the formation of singlet oxygen or other ROS would occur in the competition between molecular oxygen and Trp and Tyr residues of α-crystallin for the photoexited KNA. Thus, one can expect that under urea-denaturing conditions, the break of multimers, containing tens of monomers, and the loss of the protein spatial self-organization would significantly increase the concentration of triplet quenchers, and the contribution from Type II reactions would be severely reduced. However, our results show the formation of all oxidized residues under both native and urea-denaturing conditions in comparable quantities. Thus, the oxidation of Met and Trp residues most likely occurs via the direct reactions of KNA$^{\bullet}$ with α-crystallin residues, though a contribution from the residual oxygen cannot be completely ruled out.

From the results obtained in the present work one can make a rough estimation of the extent of decay of Trp- and Tyr-containing peptides in the anaerobic KNA-sensitized photolysis. Typically, a sample of 2.5 cm^{3} volume containing 6.0 mg ml^{-1} α-crystallin was irradiated by the light flux of approximately 3.6×10^{17} quanta per second. From the data presented in Figures 4 and S5 of SI one can estimate that for majority of Trp- and Tyr-containing peptides, the quantum yields of decomposition do not exceed 2-3%. Such low decay quantum yields confirm the conclusion drawn from the flash-photolysis data (see section 2.1.2) that the major pathway of decay of photochemically formed radicals is the restoration of the initial compounds via the back electron transfer reaction.

The protein aggregation is the major consequence of KNA-sensitized photolysis; yet the analysis of the obtained data revealed only one peptide, which can be assigned as a cross-linked peptide. Most likely, there are several sites of cross-linking, so the concentration of each individual cross-linked peptide is too low for the identification. The systematic search for the covalent cross-links in photolyzed proteins requires a special sample preparation, and it should be carried out in a separate work.

The aggregation of α-crystallin under anaerobic conditions was earlier reported for the riboflavin-sensitized photolysis using the light of visible region.[26] Flavin and its derivatives are well-known photosensitizers reacting with Trp and Tyr residues via the electron transfer mechanism.[69,70] It was shown[26] that the covalent binding of riboflavin to α-crystallin is the protein modification preceding the aggregation. It seems likely that riboflavin could be a linker between two polypeptide chains. However, our data did not reveal any evidence for the covalent attachment of KNA to α-crystallin indicating the domination of another mechanism for the protein cross-linking. Perhaps, KNA-sensitized oxidation of Trp residues plays a key role in the observed aggregation.

It has been shown earlier that the antioxidant Asc is an effective quencher of triplet states.[37] According to the results

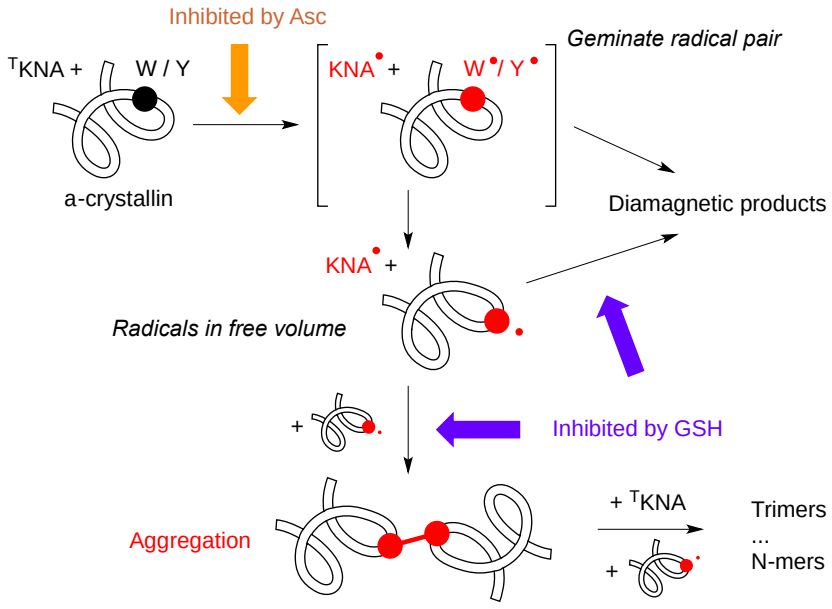

Scheme 1. Mechanism of KNA-sensitized modifications of α-crystallin in UVA photolysis under anaerobic conditions.

obtained in the present work, Asc quenches ^{T}KNA with the rate constant of 1.4×10^{9} $M^{-1}s^{-1}$. In the recent work of Linetsky et al.[28] it was shown that anaerobic irradiation of the lens UV filters (KN, 3-hydroxykynurenine, N-formylkynurenine) in the presence of Asc results in the Asc oxidation and the formation of dehydroascorbate. In the human lens, these reactions eventually lead to the accumulation of advanced glycation end products.[28,71] Based on these findings, it was suggested[28] that KN-mediated Asc oxidation might be an important mechanism for cataractogenesis. Our data testify that in fact, Asc photo-oxidation plays a protective role by quenching highly reactive triplet states of KNs and its products and by preventing their reactions with proteins. The Asc$^{\bullet}$ radical formed in the triplet quenching reaction is a significantly less reactive species than ^{T}KN or ^{T}KNA; *in vitro* it does not induce noticeable modifications in the α-crystallin structure and, most probably, decays in the radical recombination reactions. In the lens it can also be scavenged by the other antioxidant GSH. High abundance of Asc in lenses of diurnal animals as compared to nocturnal ones[72] can be considered as an additional argument speaking in favor of the protective role of Asc against the UVA radiation.

The rate constant of the triplet state quenching by GSH is at least two orders of magnitude lower than by Asc (ref.[37] and this work); however, this compound is an excellent electron donor, able to reduce free radicals up to the diamagnetic state. GS$^{\bullet}$ radicals so formed recombine in solution, forming oxidized glutathione GSSG. The inhibition of the protein aggregation in the presence of GSH confirms the proposed radical mechanism of the protein covalent cross-linking, and indicates the important role of antioxidant GSH in preventing the protein aggregation and the chemical modifications of amino acid residues.

It should be noted that the important role of Asc and GSH in the prevention of photoinduced protein modifications was demonstrated under *in vitro* conditions. In the real lens tissue the crystallin concentration is much higher, therefore the antioxidant protection from photosensitized reactions might be less effective. The abundance of UV filters and antioxidants in the human lens decreases with age and during the cataractogenesis,[31,32,48] reducing the total ability of the lens tissue to resist the photoinduced modifications of proteins. Therefore, the probability of photoinduced damages to crystallins seriously increases with the normal aging and especially with the cataract development.

4 Experimental details

4.1. Chemicals

Kynurenic acid, *L*-tryptophan, *L*-tyrosine, *L*-cysteine, *L*-methionine, *L*-histidine, *L*-phenylalanine, ascorbate and reduced glutathione were from Sigma (St. Louis, MO, USA). Chemicals used for gel electrophoresis were from Bio-Rad (Hercules, CA, USA). All chemicals used for mass spectrometry analysis were of the highest purity from Bio-Rad (Hercules, CA, USA), Amersham Biosciences (Amersham, UK) or Sigma (St. Louis, MO, USA).

4.2. Isolation of α-crystallins

Enucleated bovine eyes were obtained from a local abattoir (Novosibirsk, Russia) and delivered on ice within 12 hours after death. The extracted lenses were homogenized in phosphate buffered saline (PBS, 50 mM of phosphate salts and 100 mM of sodium chloride, pH 7.4) in the presence of the protease inhibitor cocktail (Sigma/Aldrich). The homogenate was centrifuged at 4°C at 12000×g for 30 min to remove the water-insoluble material. The soluble proteins were separated into high, medium, and low molecular mass fractions by size-exclusion chromatography using a Superdex 200 10/300 GL column from GE Healthcare (Piscataway, NJ, USA) with PBS as the mobile phase, at a flow rate of 0.5 ml/min and the detection at 280 nm. High molecular mass fractions of proteins, known as multimers of α-crystallins, were collected from several consequent chromatographic runs. HPLC-ESI-MS analysis showed that the collected fraction is a mixture of monomers of αA- and αB-crystallins and their singly and doubly phosphorylated derivatives. The amount of other polypeptides did not exceed 1% (estimated by absorption at 220 nm). In all further experiments, the concentration of α-crystallin in the samples was estimated from the absorption at 280 nm, using the molar extinction coefficient ε_{280} = 0.85 cm^2 mg^{-1}.[73]

4.3. Optical measurements

4.3.1. Steady-state absorption and fluorescence measurements

UV-visible electronic absorption spectra were recorded with an Agilent 8453 from Hewlett-Packard (La Jolla, CA, USA) spectrophotometer. Fluorescence emission spectra were measured with a FLSP920 spectrofluorimeter from Edinburgh Instruments (Edinburgh, UK). All fluorescence measurements were carried out in a 10 × 10 mm^2 quartz cell; the obtained spectra were corrected for the wavelength-dependent sensitivity of the detection.

4.3.2. Transient absorption measurements

Transient absorption spectra and kinetics were measured with the use of a nanosecond laser flash photolysis (LFP) setup described earlier.[34] Briefly, samples in a 10 × 8 mm^2 quartz cell were irradiated with a Quanta-Ray LAB-130-10 Nd:YAG laser from SpectraPhysics (Mountain View, CA, USA): 355 nm, pulse duration 8 ns, pulse energy up to 135 mJ. A fraction of the laser beam was split by a quartz plate and directed to a photodiode for triggering an oscilloscope and to a Newport 1918-C power meter (Franklin, MA, USA) for the permanent monitoring of the laser energy. The dimensions of the laser beam at the front of the cell were reduced by a diaphragm to 2.5 mm × 8 mm. The monitoring system includes a DKSh-150 xenon short-arc lamp from Stella Ltd. (Moscow, Russia) connected to a high current pulser, a Newport 78025 monochromator (Stratford, CT, USA), a 9794B photomultiplier from ET Enterprises Ltd. (Uxbridge, UK), and a WaveRunner 104MXi digital oscilloscope from LeCroy (Chestnut Ridge, NY, USA). The probe light, concentrated in a rectangle of 2.5 mm

height and 1 mm width, passed through the cell parallel to the front (laser irradiated) window. Thus, in all experiments the excitation optical length was 1 mm, and the monitoring optical length was 8 mm. All solutions were bubbled with argon for 15 minutes prior to and during irradiation.

4.3.3. Anaerobic UVA photolysis of α-crystallins

The samples containing PBS solution of 6.0 mg ml^{-1} α-crystallin and 3.0×10^{-4} M KNA in a 10 × 8 mm^2 quartz cell (sample volume 2.5 ml) were irradiated with a DRSh-1000 high-pressure mercury lamp from Stella Ltd. (Moscow, Russia). A water filter was used to cut off the infrared light, and the spectral region of 330–390 nm was selected with a set of UV glass filters. Actinometry was performed according to standard methods using the aqueous solution of potassium ferrioxalate.[74] The photon flux on the surface of the quartz cell was $(3.4 \pm 0.6) \times 10^{17}$ quanta per second.

All solutions were bubbled with argon for 15 minutes prior to and during irradiation. Before the sample irradiation and at the different time intervals of photolysis the absorption spectra of samples were recorded and the aliquots of 50 µl were taken with a syringe for subsequent analysis.

4.4. Gel electrophoresis

The aliquots of α-crystallin solution taken before and during UVA photolysis were subjected to SDS-PAGE by the method of Laemmli[75] using 15% polyacrylamide gels (10×10 cm). Before electrophoresis, all samples were treated for 5 minutes with 31 mM Tris-HCl containing 1% SDS in the presence of 2.5% β-mercaptoethanol at 95°C. After electrophoresis, the gels were stained with Coomassie blue R-250 in 10% acetic acid. Gel images were obtained using a VersaDoc 4000 MP Imaging System from Bio-Rad (Hercules, CA, USA). The approximate molecular masses of proteins under study were determined using the protein markers from ThermoScientific (Vilnius, Lithuania) and Quantity One software for VersaDoc system.

4.5. Purification and tryptic digestion of α-crystallins after UVA photolysis

The protein aliquots taken during the UVA photolysis were purified from KNA and other low molecular mass molecules by Amicon Ultra centrifugal filters from Merck Millipore (Tullagreen, Ireland) with the molecular mass cut-off 3 kDa. Typically, 25 µl of aliquot were diluted by 40 mM ammonium bicarbonate buffer (AmB, pH 8.0) up to the volume of 400 µl and centrifuged at 4°C at 10000×g for 20 minutes. The concentrated sample was diluted and centrifuged as mentioned above two more times; the final volume of the protein solution was approximately 150 µl. Then the absorption and fluorescence spectra of irradiated α-crystallins were recorded.

The enzymatic hydrolysis of the irradiated α-crystallins was carried out with trypsin. The purified proteins (5 µl) were diluted in 40 mM AmB (45 µl) and subjected to the overnight digestion at 37°C. The trypsin concentration was 0.2 µg per digest. The obtained peptides were analyzed by HPLC-ESI-MS.

The aggregated α-crystallins were analyzed using MALDI-TOF-MS and HPLC-ESI-MS analyses. The protein-containing bands were manually excised from the gel and destained three times with 200 mM AmB in 50% acetonitrile (ACN) at 37°C for 30 min. The gel pieces were dehydrated in 100% ACN and then digested by trypsin (10 µl, 0.2 µg trypsin in 40 mM AmB per sample) at 37°C for 16 h. The extracted peptides were desalted and concentrated on C18 ZipTip Pipette Tips from Millipore (Billerica, MA, USA), eluted with 1 µl ACN and dissolved in 20 µl water. The resulting peptide solution was used for the subsequent MALDI-TOF-MS and HPLC-ESI-MS analysis.

4.6. Mass spectrometry analysis

4.6.1. MALDI-TOF-MS measurements

Digested proteins from the gel were analyzed with the use of a MALDI-TOF Ultraflex III TOF/TOF mass spectrometer from Bruker Daltonics (Bremen, Germany). The tryptic peptides extracted from the gel (1 µl) were mixed with a saturated solution (1 µl) of 2,5-dihydroxybezoic acid in aqueous 70% ACN / 0.1% trifluoroacetic acid and spotted onto a standard MTP384 ground steel target plate. The mass spectra were acquired in a positive ion mode in the *m/z* range of 600-6000. The instrument calibration was performed with the standard mixture of peptides from Bruker Daltonics (Bremen, Germany). The calibration was verified by internal *m/z* peaks arising from the trypsin autolysis. The mass spectra were analyzed using FlexAnalysis software 3.0, Build 96 from Bruker Daltonics (Bremen, Germany), and the peptide masses were submitted to a local Mascot search engine for the protein identification.

4.6.2. HPLC-ESI-MS measurements

HPLC-ESI-MS analysis was performed with an ESI-q-TOF high-resolution hybrid mass spectrometer maXis 4G from Bruker Daltonics (Bremen, Germany) connected to HPLC system UltiMate 3000RS from Dionex (Germering, Germany), equipped with a flow cell UV-Vis diode array detector (DAD). The HPLC separations were performed on Agilent Zorbax 300SB-C18 (1.0 × 150 mm, 300 Å, 3.5 µm) column with mobile phases A (0.1% formic acid in water) and B (0.1% formic acid in ACN) at a flow rate of 150 µl/min. Proteins were separated with the gradient: 5% B (0-4 min), 5%–30% B (4-5 min), 30%–50% B (5-45 min) and 50%–95% B (45-46 min). Peptide separations were performed with the gradient: 5% B (0-5 min), 5%–60% B (5-45 min) and 60%–95% B (45-46 min).

The ESI-MS analysis was performed as described in detail in ref.[76] Mass spectra were acquired in the positive mode in the m/z range of 300-2900. The instrument parameters were set as follows: end plate offset -500 V; capillary voltage 4000 V; nebulizer pressure 1 bar; dry gas flow 6 l/min; dry gas temperature 200 °C. The MS calibration was performed by the injection of an ESI-L low concentration tuning mix from Agilent Technologies (Santa Clara, CA, USA) for proteins and a sodium formate cluster calibration solution for peptides. Every HPLC-ESI-MS measurement contained a time segment with the MS calibration data, used for the instrument parameter control and for the post-recalibration of the sample data if necessary. The intensities of peptide signals were measured in the MS

scan; the amino acid sequence of the selected peptides was reconstructed using automatic MS/MS mode with collision induced dissociation (CID) fragmentation. The typical accuracy of the mass measurement was ± 0.001 Da and the typical resolution was 50 000. The obtained data were analyzed with DataAnalysis software 4.0 and QuantAnalysis software 2.0 from Bruker Daltonics (Bremen, Germany), and the peptide masses were submitted to a local Mascot search engine for protein identification.

4.6.3. Protein identification

The monoisotopic peptide masses obtained in MALDI-TOF-MS and HPLC-ESI-MS experiments were compared with the theoretical masses for bovine α-crystallin tryptic peptides available in the SwissProt database (http://us.expasy.org, 2015) using the local Mascot 2.2.04 searching engine. One missed cleavage and a maximum mass error of 50 ppm for MALDI-TOF-MS and 1 ppm for HPLC-ESI-MS data were allowed in the search. N-terminal protein acetylation (+42), phosphorylation of threonine and serine (+80), and methionine oxidation (+16) were specified as variable modifications. The identification was considered positive when the highest-scoring protein entry was statistically significant ($p < 0.05$) and at least four peptides have been identified.

Conclusions

The aggregation of proteins is the major outcome of the UVA photolysis of α-crystallin under anaerobic conditions in the presence of KNA. Other consequences of photosensitized reactions are the degradation of Trp and Tyr residues, the oxidation of Met and Trp residues, and the formation of UVA absorbing protein modifications. Our data indicate that the oxidation of amino acid residues should be attributed to the reactions between KNA• radicals and radicals of amino acid residues resulting in the oxygen transfer from KNA to a residue. Asc, being the effective quencher of triplet molecules, inhibits all initial reactions of KNA triplets with Trp- and Tyr-residues of α-crystallin, while GSH, being the effective scavenger of free radicals, reacts with the radicals formed in KNA-sensitized reactions. The obtained results testify that photochemical reactions of the products of thermal and photochemical degradation of natural UV filters can induce the protein aggregation, the oxidation of amino acid residues and the formation of products with blue fluorescence. The efficiency of these processes in the human lens is rather low due to the low abundance of these photosensitizing products and high concentrations of antioxidants. However, the UVA-induced changes in the crystallin structure can accumulate in significant amounts during the lifespan of an individual, and give a substantial contribution to the development of cataract.

Acknowledgements

This work was supported by the Russian Scientific Foundation (grant №14-14-00056). The MS measurements were performed with the financial support from the Russian Foundation for Basic Research (Projects № 14-03-31189 and 14-03-00027) and the grant from the President of Russian Federation (Project MK-5367.2015.3). Authors thank Dr. Sergey V. Kulemzin (Institute of Molecular and Cell Biology, Novosibirsk, Russia) for the help with the crystallin separation.

References

1 L.R. Miesbauer, X. Zhou, Zhu. Yang, Zhi. Yang, Y. Sun, D.L. Smith, J.B. Smith. *J. Biol. Chem.*, 1994, **269**, 12494.
2 A.L. Lund, J.B. Smith, D.L. Smith. *Exp. Eye Res.*, 1996, **63**, 661.
3 P.G. Hains, R.J.W. Truscott. *J. Proteome Res.*, 2007, **6**, 3935.
4 K.K. Sharma, P. Santhoshkumar. *Biochim. Biophys. Acta*, 2009, **1790**, 1095.
5 R. Truscott. *J. Clinic Experiment. Ophthalmol.*, 2013, **S1**:008.
6 P.J. Dolin. *Br. J. Ophthalmol.*, 1994, **78**, 478.
7 D. Balasubramanian *J. Ocul. Pharmacol. Ther.*, 2000, **16**, 285.
8 S.D. Varma, S. Kovtun, K.R. Hegde. *Eye Contact Lens*, 2011, **37**, 233.
9 S. Zigman. *Optometry Vision Sci.*, 1995, **72**, 899.
10 E.R. Gaillard, L. Zheng, J.C. Merriam, J. Dillon. *Invest. Ophthalmol. Vis. Sci.*, 2000, **41**, 1454.
11 K.L. Bergauer, J.F.R. Kuck, K.C. Su, N.-T. Yu. *Int. Contact Lens Clin.*, 1991, **18**, 182.
12 F.J. Giblin, V.R. Leverenz, V.A. Padgaonkar, N.J. Unakar, L. Dang, L.R. Lin, M.F. Lou, V.N. Reddy, D. Borchman, J.P. Dillon. *Exp. Eye Res.*, 2002, **75**, 445.
13 M.F. Simpanya, R.R. Ansari, V. Leverenz, F.J. Giblin. *Photochem. Photobiol.*, 2008, **84**, 1589.
14 F.J. Giblin, L.R. Lin, M.F. Simpanya, V.R. Leverenz, C.E. Fick. *Exp. Eye Res.*, 2012, **102**, 17.
15 F.P. Gasparro. *Environ. Health Perspect.*, 2000, **108**, 71.
16 G.T. Wondrak, M.K. Jacobson, E.L. Jacobson. *Photochem. Photobiol. Sci.*, 2006, **5**, 215.
17 D.I. Pattison, A.S. Rahmanto, M.J. Davies. *Photochem. Photobiol. Sci*., 2012, **11**, 38.
18 M. Bando, I. Mikuni, H. Obasava. *Exp. Eye Res.*, 1982, **34**, 953.
19 M. Bando, N.T. Yu, J.F.R. Kuck. *Invest. Ophthalmol. Vis. Sci.*, 1984, **25**, 581.
20 M. Linetsky, H.L. James, B.J. Ortwerth. *Exp. Eye Res.*, 1996, **63**, 67.
21 J. Dillon, M. Skonieczna, K. Mandalm, D.C. Paik. *Photochem. Photobiol*., 1999, **69**, 248.
22 M.J. Davies, R.J.W. Truscott. *J. Photochem. Photobiol. B: Biol.*, 2001, **63**, 114.
23 N.R. Parker, J.F. Jamie, M.J. Davies, R.J.W. Truscott. *Free Rad. Biol. Med.*, 2004, **37**, 1479.
24 J. Mizdrak, P.G. Hains, R.J.W. Truscott, J.F. Jamie, M.J. Davies. *Free Rad. Biol. Med.*, 2008, **44**, 1108.
25 S.D. Varma, K.R. Hegde. *Mol. Cell Biochem.*, 2010, **340**, 49.
26 R. Ugarte, A.M. Edwards, M.S. Diez, A. Valenzuela, E. Silva. *J. Photochem. Photobiol. B: Biol.* 1992, **13**, 161.
27 L.A. Ervin, J. Dillon, E.R. Gaillard. *Photochem. Photobiol.*, 2001, **73**, 685.
28 M. Linetsky, C.T. Raghavan, K. Johar, X.J. Fan, V.M. Monnier, A.R. Vasavada, R.H. Nagaraj. *J. Biol. Chem.*, 2014, **289**, 17111.
29 R. McNulty, H. Wang, R.T. Mathias, B.J. Ortwerth, R.J. Truscott, S. Bassnett. *J. Physiol.*, 2004, **559**, 883.
30 A.M. Wood, R.J.W. Truscott. *Exp. Eye Res.*, 1993, **56**, 317.
31 L.M. Bova, M.H. Sweeney, J.F. Jamie, R.J.W. Truscott. *Invest. Ophthalmol. Vis. Sci.*, 2001, **42**, 200.
32 I.M. Streete, J.F. Jamie, R.J.W. Truscott. *Invest. Ophthalmol. Vis. Sci.*, 2004, **45**, 4091.

33 O.A. Snytnikova, A.Z. Fursova, E.I. Chernyak, V.G. Vasiliev, S.V. Morozov, N.G. Kolosova, Yu.P. Tsentalovich. *Exp. Eye Res.*, 2008, **86**, 951.
34 Yu.P. Tsentalovich, P.S. Sherin, L.V. Kopylova, I.V. Cherepanov, J. Grilj, E. Vauthey. *Invest. Ophthalmol. Vis. Sci.*, 2011, **52**, 7687.
35 Yu.P. Tsentalovich, O.A. Snytnikova, P.S. Sherin, M.D.E. Forbes. *J. Phys. Chem. A*, 2005, **109**, 3565.
36 P.S. Sherin, Yu.P. Tsentalovich, O.A. Snytnikova, R.Z. Sagdeev. *J. Photochem. Photobiol. B: Biol.*, 2008, **93**, 127.
37 O.A. Snytnikova, P.S. Sherin, L.V. Kopylova, Yu.P. Tsentalovich. *Rus. Chem. Bull.*, 2007, **56**, 732.
38 L.M. Taylor, J.A. Aquilina, J.F. Jamie, R.J.W. Truscott. *Exp. Eye Res.*, 2002, **75**, 165.
39 Yu.P. Tsentalovich, O.A. Snytnikova, M.D.E. Forbes, E.I. Chernyak, S.V. Morozov. *Exp. Eye Res.*, 2006, **83**, 1439.
40 L.M. Taylor, J.A. Aquilina, J.F. Jamie, R.J.W. Truscott. *Exp. Eye Res.*, 2002, **74**, 503.
41 A. Korlimbinis, R.J.W. Truscott. *Biochemistry*, 2006, **45**, 1950.
42 B.K. Zsizsik, R. Hardeland. *Comp. Biochem. Physiol. C*, 2002, **133**, 383.
43 T. Zarnowski, R. Rejdak, Y. Zagorski, A.G.M. Juenemann, E. Zrenner, T. Kocki, E.M. Urbanska, W.A. Turski. *Ophthalm. Res.*, 2004, **36**, 124.
44 T. Zarnowski, R. Rejdak, E. Zielinska-Rzecka, E. Zrenner, P. Grieb, Z. Zagórski, A. Juenemann, W.A. Turski. *Curr. Eye Res.*, 2007, **32**, 27.
45 P.S. Sherin, N.P. Gritsan, Yu.P. Tsentalovich. *Photochem. Photobiol. Sci*., 2009, **8**, 1550.
46 P.S. Sherin, J. Grilj, L.V. Kopylova, V.V. Yanshole, Yu.P. Tsentalovich, E. Vauthey, *J. Phys. Chem. B*, 2010, **114**, 11909.
47 E.A. Zelentsova, P.S. Sherin, O.A. Snytnikova, R. Kaptein, E. Vauthey, Yu.P. Tsentalovich. *Photochem. Photobiol. Sci*., 2013, **12**, 546.
48 Yu.P. Tsentalovich, T.D. Verkhovod, V.V. Yanshole, A.S. Kiryutin, L.V. Yanshole, A.Z. Fursova, D.A. Stepakov, V.P. Novoselov, R.Z. Sagdeev. *Exp. Eye Res.*, 2015, **134**, 15.
49 A. Korlimbinis, J.A. Aquilina, R.J.W. Truscott. *Exp. Eye Res.*, 2007, **85**, 219.
50 O.A. Snytnikova, A.Z. Fursova, E.I. Chernyak, V.G. Vasiliev, S.V. Morozov, N.G. Kolosova, Yu.P. Tsentalovich. *Exp. Eye Res.*, 2008, **86**, 951.
51 H. Heath. *Exp. Eye Res.*, 1962, **1**, 362.
52 F.J. Giblin. *J. Ocul. Pharmacol. Ther.*, 2000, **16**, 121.
53 D.L. Williams. *Veterinary Ophthalmol.*, 2006, **9**, 292.
54 M.P. Pileni, M. Giraud, R. Santus. *Photochem. Photobiol.*, 1979, **30**, 251.
55 K. Kawahara, Ch. Tanford. *J. Biol. Chem.*, 1966, **241**, 3228.
56 D.V. Bent, E. Hayon. III. Tryptophan. *J. Am. Chem. Soc.*, 1975, **97**, 2612.
57 F.D. Bryant, R. Santus, L.I. Grossweiner. *J. Phys. Chem.*, 1975, **79**, 2711.
58 Yu.P. Tsentalovich, O.A. Snytnikova, R.Z. Sagdeev. *J. Photochem. Photobiol. A: Chem.*, 2004, **162**, 371.
59 R.J.W. Truscott. *Exp. Eye Res.*, 2005, **80**, 709.
60 Ø. Risa, O. Sæther, S. Löfgren, P.G. Söderberg, J. Krane, A. Midelfart. *Invest. Ophthalmol. Visual Sci.*, 2004, **45**, 1916.
61 Ø. Risa, O. Sæther, M. Kakar, V. Mody, S. Lofgren, P.G. Soderberg, J. Krane, A. Midelfart. *Exp. Eye Res.*, 2005, **81**, 407.
62 M.N. Ayala, R. Michael, P.G. Soderberg. *Invest. Ophthalmol. Visual Sci.*, 2000, **41**, 3539.
63 M.N. Ayala, R. Michael, P.G. Soderberg. *Exp. Eye Res.*, 2000, **70**, 451.
64 K. Mafia, R. Gupta, M. Kirk, L. Wilson, O.P. Srivastava, S. Barnes. *Mol. Vis.*, 2008, **14**, 234.
65 P.S. Sherin, J. Grilj, Yu.P. Tsentalovich, E. Vauthey. *J. Phys. Chem. B*, 2009, **113**, 4953.
66 M.P. Pileni, M. Giraud, R. Santus. *Photochem. Photobiol.*, 1979, **30**, 257.
67 M. Stuart-Audette, Y. Blouquit, M. Faraggi, C. Sicard-Roselli, C. Houee-Levin, P. Jolle. *Eur. J. Biochem.*, 2003, **270**, 3565.
68 O.B. Morozova, P.J. Hore, R.Z. Sagdeev, A.V. Yurkovskaya. *J. Phys. Chem. B*, 2005, **109**, 21971.
69 G. Viteri, A.M. Edwards, J. De la Fuente, E. Silva. *Photochem. Photobiol.* 2003, **77**, 535.
70 P.P. Levin, A.S. Tatikolov, I.G. Panova, N.B. Sul'timova. High Energy Chem. 2010, **44**, 216.
71 G.L. Simpson, B.J. Ortwerth. *Biochim. Biophys. Acta*, 2000, **1501**, 12.
72 G.R. Reiss, P.G. Werness, P.E. Zollman, R.F. Brubaker. *Arch. Ophthalmol.*, 1986, **104**, 753.
73 T. Putilina, F. Skouri-Panet, K. Prat, N.H. Lubsen, A. Tardieu. *J. Biol. Chem.*, 2003, **278**, 13747.
74 J.R. Calvert, J.N. Pitts. Photochemistry. John Willey, Springer, 1969.
75 U.K. Laemmli. *Nature*, 1970, **227**, 680.
76 V.V. Yanshole, O.A. Snytnikova, A.S. Kiryutin, L.V. Yanshole, R.Z. Sagdeev, Yu.P. Tsentalovich. *Exp. Eye Res.*, 2014, **125**, 71.